Journal Pre-proofs

Design, synthesis and biological evaluation of novel osthole-based derivatives as potential neuroprotective agents

Li Zhang, Yuhang Wu, Guixiang Yang, Haixian Gan, Dayong Sang, Jiye Zhou, Lin Su, Rui Wang, Lei Ma

PII: S0960-894X(20)30744-7
DOI: https://doi.org/10.1016/j.bmcl.2020.127633
Reference: BMCL 127633

To appear in: *Bioorganic & Medicinal Chemistry Letters*

Received Date: 25 August 2020
Revised Date: 13 October 2020
Accepted Date: 16 October 2020

Please cite this article as: Zhang, L., Wu, Y., Yang, G., Gan, H., Sang, D., Zhou, J., Su, L., Wang, R., Ma, L., Design, synthesis and biological evaluation of novel osthole-based derivatives as potential neuroprotective agents, *Bioorganic & Medicinal Chemistry Letters* (2020), doi: https://doi.org/10.1016/j.bmcl.2020.127633

Design, synthesis and biological evaluation of novel osthole-based derivatives as potential neuroprotective agents

Li Zhang [a, †], Yuhang Wu [a, †], Guixiang Yang [a, †], Haixian Gan [a], Dayong Sang [b], Jiye Zhou [a], Lin Su [a], Rui Wang [a, *], Lei Ma [a, *]

[a] *Shanghai Key Laboratory of New Drug Design, School of Pharmacy, East China University of Science and Technology, 130 Meilong Road, Shanghai 200237, China*

[b] *College of Chemical Engineering and Pharmacy, Jingchu University of Technology, Jingmen, Hubei 448000, China*

†These authors contributed equally to this work.

* Corresponding authors. Tel.: +86 2164253691; Fax: +86 2164253691.

E-mail addresses: malei@ecust.edu.cn (L. Ma), ruiwang@ecust.edu.cn (R. Wang)

Abstract:

A total of 26 compounds based on osthole skeleton were designed, synthesized. Their cytoprotective abilities of antioxidation, anti-inflammation and $A\beta_{42}$ (Amyloid β-protein 42) -induced neurotoxicity were evaluated by MTT assays. Mechanism of the action of selected compounds were investigated by molecular docking. AlogP, logS and blood-brain barrier (BBB) permeability of all these compounds were simulated by admetSAR. Most of the compounds showed better antioxidative and anti-inflammatory activities compared with osthole, especially **OST7** and **OST17**. The compound **OST7** showed relative high activity in neuroprotection against H_2O_2 (45.7 ± 5.5 %), oxygen glucose deprivation (64.6 ± 4.8 %) and $A\beta_{42}$ (61.4 ± 5.2 %) at a low concentration of 10 μM. EC_{50} of selected compounds were measured in both H_2O_2 and OGD induced cytotoxicity models. Moreover, NO inhibiting ability of **OST17**(50.4 ± 7.1 %) already surpassed the positive drug indomethacin. The structure activity relationship study indicated that introduction of piperazine group, tetrahydropyrrole group and aromatic amine group might be beneficial for enhancement of osthole neuroprotective properties. Molecular docking explained that the reason **OST7** exhibited relatively stronger neuroprotection against Aβ because of the greater area of interactions between molecule and target protein. **OST7** and **OST17** both provided novel methods to investigate osthole as anti-AD drugs.

Keywords: Osthole; Neuroprotection; Antioxidant; Anti-inflammation; Amyloid β-protein, Molecular docking.

Alzheimer's disease, also referred to as AD, is a neurodegenerative disease, which is usually caused by the chronic damages of neurons and worsens over time.[1,2] The most common initial symptom is memory deficit.[1] As the disease progresses, other symptoms may include but not limited to oral presentation difficulties, mobility problems, mood swings and disorientation.[1,3] Progressive loss of physiological functions may eventually lead to death.[4] According to recent research, AD is the sixth leading cause of death in the United States and the fifth leading cause of death among people 65 and older.[5] Unless significant breakthroughs in medicine are made, the number of people 65 and older with AD could rise from 5.5 million to 13.8 million by 2050 (almost as 3 times as current) by predictions. Meanwhile, total cost for medical care and long-term care are expected to exceed $1.1 trillion.[6] Thus, there is an urgent need for a better therapeutic strategy for AD.

The pathology of AD still remains uncertain.[7] Mainstream hypotheses include amyloid hypothesis, cholinergic hypothesis, inflammatory hypothesis, etc.[8-10] On the one hand, Excess ROS, including hydroxyl radical (·OH), hydrogen peroxide (H_2O_2), superoxide radical ($\cdot O^{-2}$), can cause damages to mitochondrial membrane and the DNA strands which maintain the normal cytofunctions.[11] On the other hand, severe inflammatory responses happened in the nidus. [12] Any factor that can cause tissue and cell damage can cause inflammation, and these factors are collectively called inflammatory mediators. Study showed almost all AD patients were accompanied by varying degrees of amyloid β-protein (Aβ) plaques accumulation in brain.[13] Another research showed the synthesis and release of multiple inflammatory mediators,

including interleukin and tumor necrosis factor (TNF), involved by Aβ,[14] illustrating the aggregation of Aβ promoted the magnitude of inflammatory responses and then added to condition aggravation. Molecular design strategy should be adapted to these mechanisms.

Osthole, one kind of furanocoumarins isolated from *Cnidium monnieri* (L.) *Cuss*., was reported to have extensive pharmacological activities, such as anti-inflammatory and antioxidant.[15] A recent research indicated osthole showed activities in neuroprotection against oxygen and glucose deprivation (OGD) by regulating the expression of mitogen-activated protein kinase (MAPK) proteins.[16] Another research showed Aβ levels can be reduced by osthole through up-regulation of miRNA-107.[17] These all revealed that osthole is a promising skeleton for developing anti-Alzheimer's drugs.

In the work presented herein, the design and synthesis of osthole derivatives were described. In our previous work, we designed sarsasapogenin and diosgenin carbamate derivatives as antioxidants. Phenyl carbamate as potent inflammation inhibitors are reported in neuroprotective drug design.[18] Thus, 4 new compounds were prepared **OST1-OST4** (Scheme 1). We also noticed the introduction of aromatic amine and piperazine were frequently applied as antioxidants and anti-inflammatory agents,[19-22] so we designed other 14 new compounds **OST5-OST18** (Scheme 2, Scheme 3). In order for further exploration of promising skeletons for neuroprotection, we synthesized columbianetin (CBN) from osthole. CBN shows an activity in anti-inflammatory properties but there have been no reports of its neuroprotection yet.[23-25]

Resveratrol, a widely known nature product possesses both anti-inflammation and antioxidation,[26] contains the structure of toluylene. Keep this in mind, we synthesized 8 new compounds **OST19-OST26** (Scheme 4) based on CBN. All synthesis strategy was show in Figure 1.

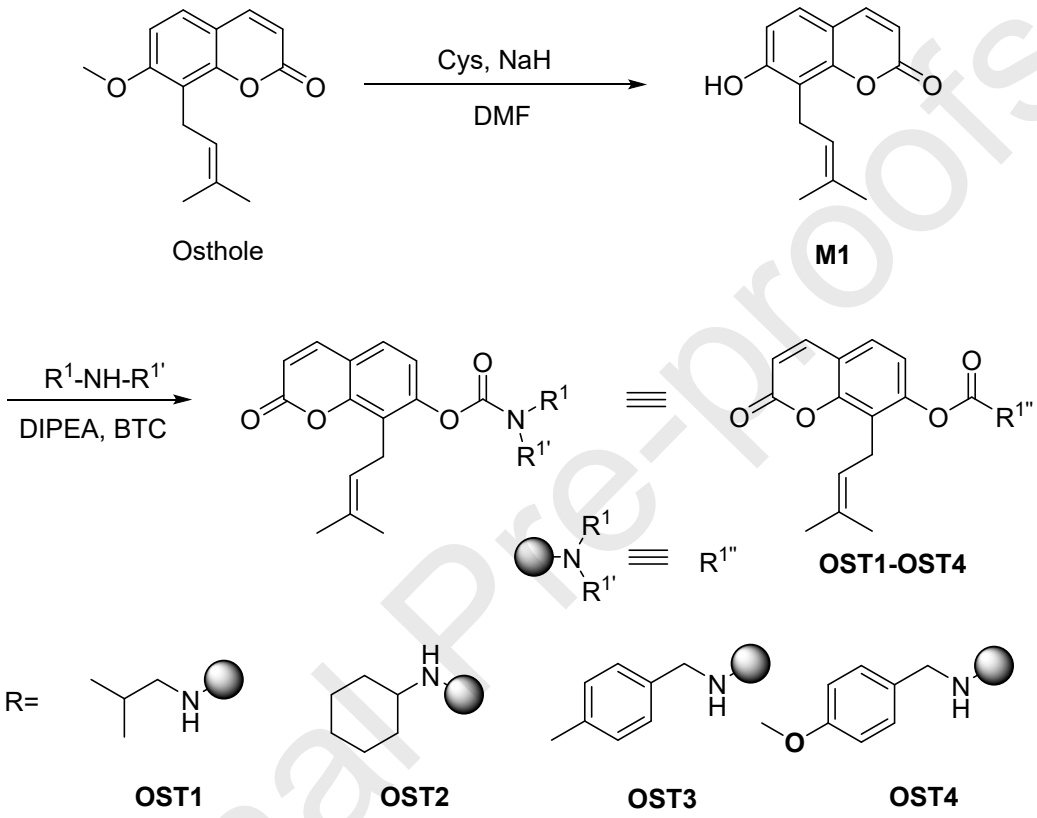

Scheme 1. Synthesis of **OST1-OST4**

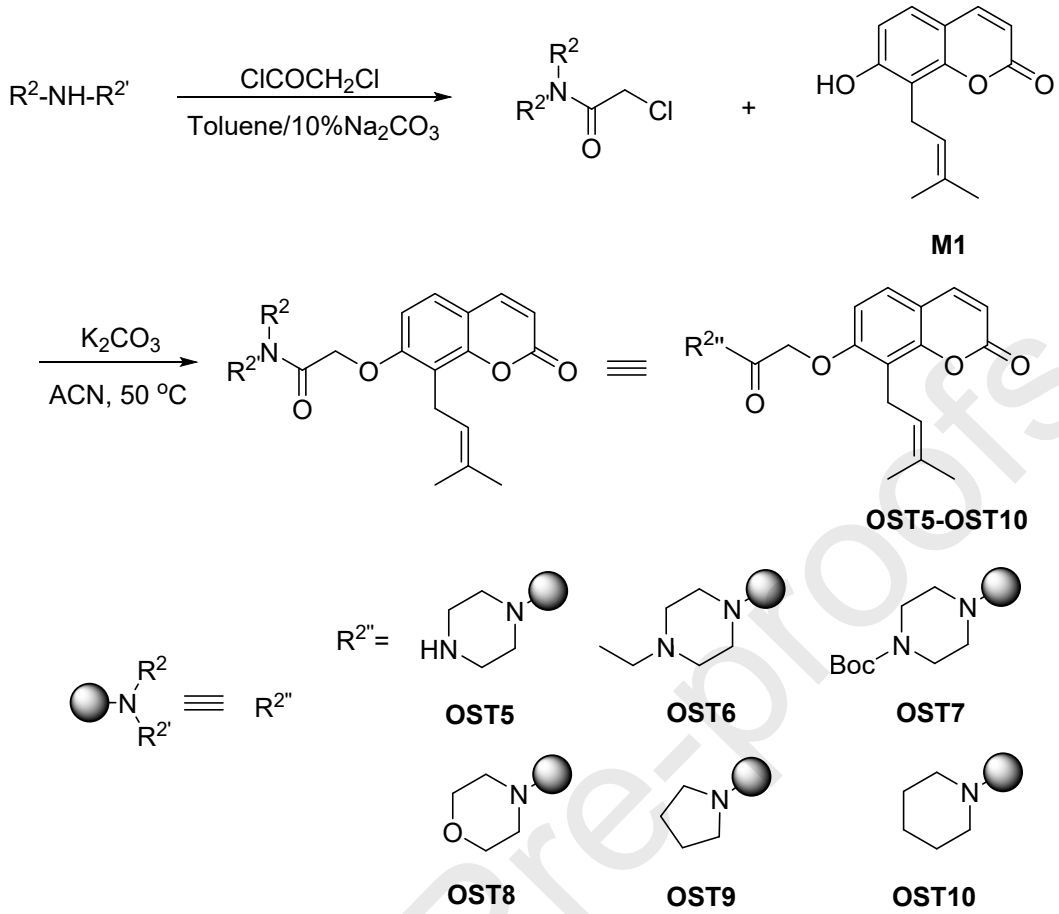

Scheme 2. Synthesis of **OST5-OST10**

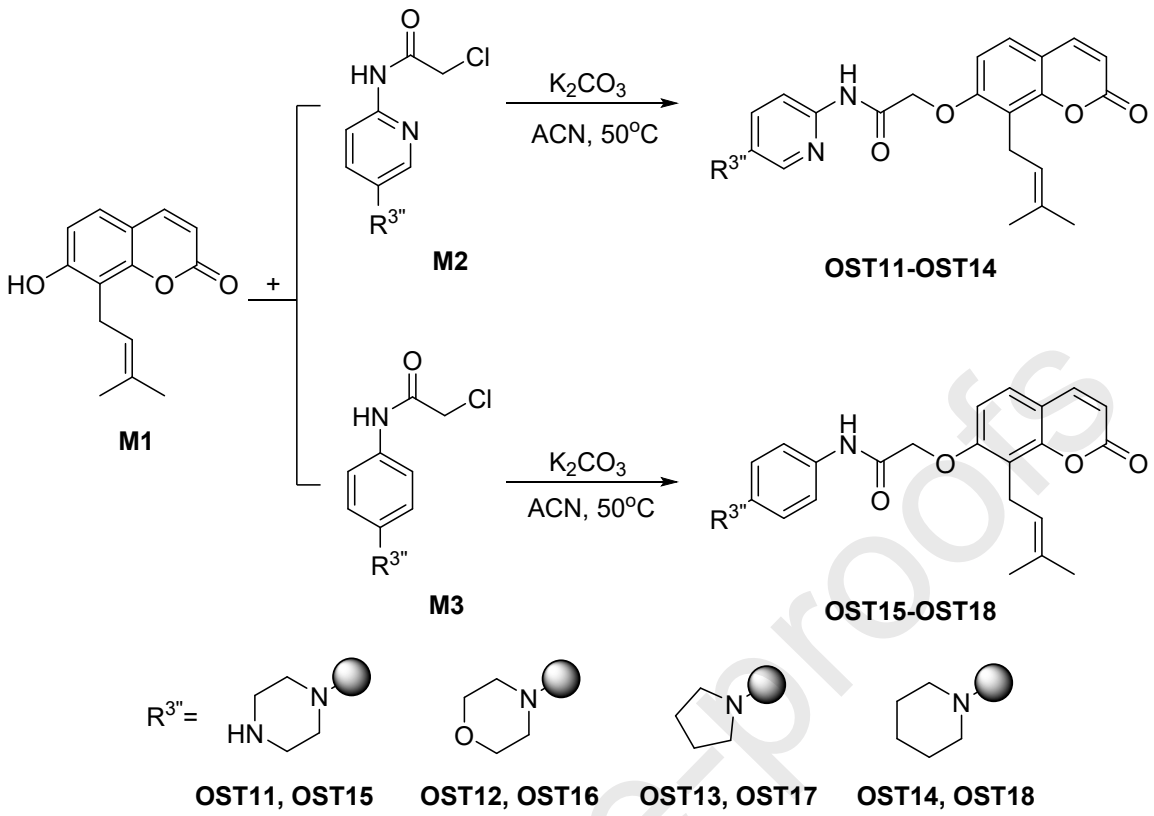

Scheme 3. Synthesis of **OST11-OST18**

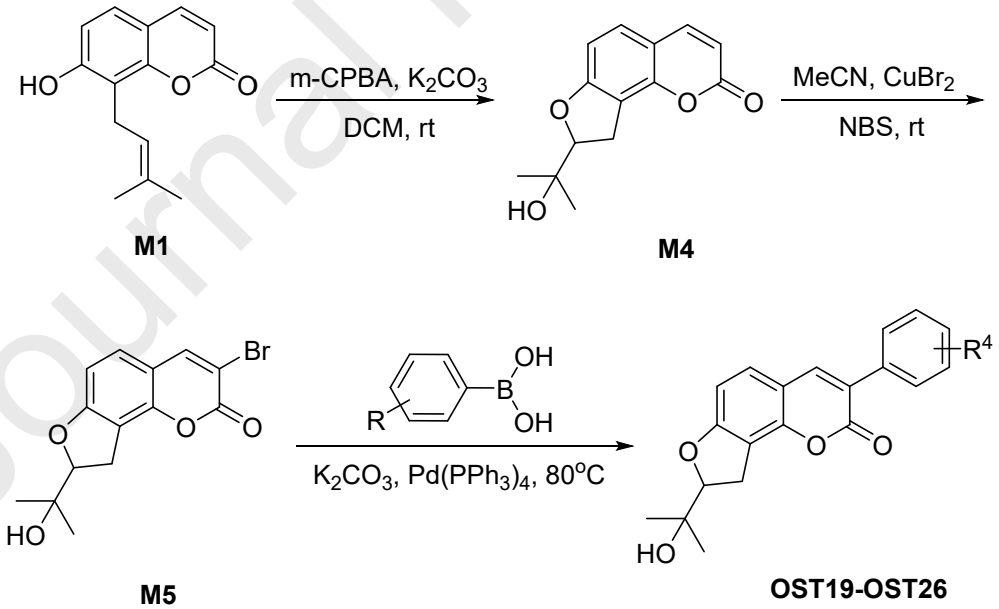

Scheme 4. Synthesis of **OST19-OST26**

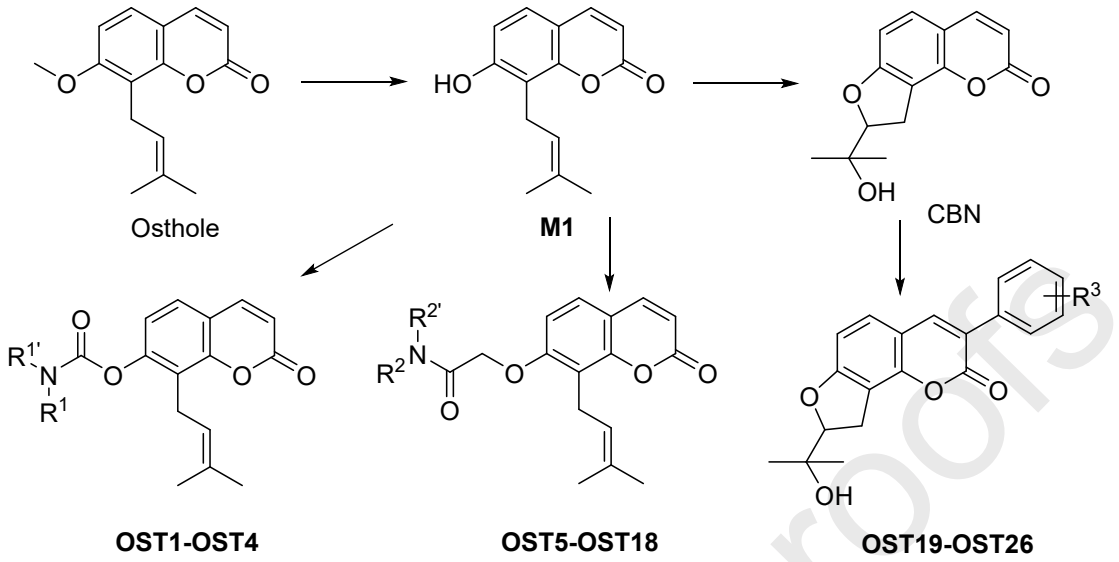

Figure 1. The synthesis strategy of target compounds.

Furanocoumarins including osthole are known to be relatively less soluble in water,[27] which hampers their druggability for oral drug. To achieve optimal brain penetration for CNS-targeted drugs, relatively high lipophilicity is preferred. Thus, AlogP, logS and blood-brain barrier (BBB) permeability of all these compounds were simulated by admetSAR (http://lmmd.ecust.edu.cn/admetsar2/, developed by Yang from ECUST). The results were listed in Table 1. As we can see, all these compounds exhibited a better BBB permeability than osthole in simulation. The introduction of nonpolar groups enhanced the hydrophobicity of osthole. Unsubstituted at one end of piperazine showed the highest value (**OST5**: -3.160, **OST11**: -3.309, **OST15**: -3.329) compared with other similar derivatives. Illustrated that the solubility can be improved by introducing basic amines. The ALogP value were all less than 5, which in accordance with Lipinski's Rule of Five.[28]

Compd.	BBB permeant probability	ALogP	LogS
osthole	0.7675	3.31	-4.372
OST1	0.9221	4.05	-4.117
OST2	0.9510	4.72	-4.153
OST3	0.9221	4.90	-3.862
OST4	0.9237	4.60	-3.660
OST5	0.9459	2.11	-3.160
OST6	0.9729	2.84	-3.674
OST7	0.9736	3.76	-3.581
OST8	0.9756	2.54	-3.247
OST9	0.9788	3.30	-3.132
OST10	0.9756	3.69	-3.247
OST11	0.9074	3.12	-3.309
OST12	0.9564	3.55	-3.528
OST13	0.9536	4.31	-3.382
OST14	0.9564	4.70	-3.528
OST15	0.9165	3.73	-3.239
OST16	0.9627	4.16	-3.556
OST17	0.9606	4.92	-3.446
OST18	0.9627	5.31	-3.556
OST19	0.8794	3.53	-3.935
OST20	0.8794	3.84	-4.164
OST21	0.8380	3.54	-4.110
OST22	0.8380	3.54	-4.110
OST23	0.9696	3.67	-4.388
OST24	0.9696	3.67	-4.388
OST25	0.9696	3.67	-4.388
OST26	0.9631	4.55	-4.503

Table 1. Physicochemical properties of compounds in silico including BBB permeant probability, ALogP and LogS

In order to evaluate the neuroprotective activity of osthole derivatives, cell viabilities

of **OST1-OST26** against oxidative stress induced by H_2O_2 in SH-SY5Y cells were carried out by MTT assay. As shown in Table 2, most tested compounds could exhibit cytoprotective properties. Carbamates have been frequently applied in cytoprotection, but unfortunately, direct introduction of carbamate groups into osthole as **OST1-4** did not bring a significant enhancement of cell viabilities. In the comparison between **OST5-7** and **OST1-4** we found that introducing piperazines into osthole increased cell viabilities more than introducing carbamates. Compound **OST7**, which possesses both carbamate and piperazine structure, was superior to other piperazine derivatives (**OST5**, **OST6**) in cytoprotection. This result accord with previous experiences and it demonstrated that the introduction position of carbamates could bring wide differences in bioactivities. When the piperazine group was replaced by morpholine and piperidine, one compound obtained (**OST8**) exhibited a similar antioxidative ability due to the similar electron density but the other derivative (**OST10)** did not give a satisfactory result. Interestingly, when the piperidine group was replaced by tetrahydropyrrole, which makes the ring smaller, the obtained **OST9** showed a better cytoprotective ability. Comparing between **OST11-14** or **OST15-18** revealed same situation that the introduction of piperazine and morpholine could both increase cell viabilities, and so do the tetrahydropyrrole. Comparing between **OST5**, **OST11**, **OST15**; **OST8**, **OST12**, **OST16**; **OST9**, **OST17** or **OST10**, **OST14**, **OST18** (we can temporarily divide them into 4 series) revealed aromatic amine did work as groups that enhanced cell viabilities. Pyridinamines (**OST11-14**) added more cytoprotective properties to osthole than phenyl amines (**OST15-18**). This might be relevant to electron cloud distributions of

aromatic rings. When it comes to the designed novel skeleton, para substituted benzene ring, with weather electron-donating groups (**OST20**, **OST21**) or electron-withdrawing groups (**OST23**, **OST26**), did not display satisfactory activities. However, ortho or meta substituted benzene ring could both increase the cytoprotective activities when compared to compound **OST19**. In summary, 18 compounds (**OST4-9, OST11-17, OST19** and **OST22-25**) exhibited good cytoprotective abilities against H_2O_2 were selected for further studies.

Compd.	Neuroprotection (%) (10μM)		Compd.	Neuroprotection (%) (10μM)	
	H_2O_2	OGD		H_2O_2	OGD
NAC	1 mM: 37.1 ± 2.5	1 mM: 84.3 ± 6.7	**OST13**	45.2 ± 4.5	58.2 ± 1.7
Osthole	23.2 ± 1.7	28.6 ± 2.3	**OST14**	32.7 ± 3.6	16.8 ± 2.1
OST1	NA	-	**OST15**	22.5 ± 1.9	8.4 ± 2.5
OST2	13.0 ± 1.6	-	**OST16**	39.5 ± 1.9	13.2 ± 1.2
OST3	NA	-	**OST17**	47.7 ± 2.1	63.4 ± 7.3
OST4	28.7 ± 2.6	35.0 ± 4.4	**OST18**	12.5 ± 1.8	-
OST5	29.2 ± 3.2	28.2 ± 2.1	**OST19**	19.7 ± 2.5	23.2 ± 3.3
OST6	33.7 ± 2.9	48.0 ± 3.7	**OST20**	18.2 ± 2.3	-
OST7	45.7 ± 5.5	64.6 ± 4.8	**OST21**	NA	-
OST8	31.5 ± 1.6	23.2 ± 4.2	**OST22**	31.0 ± 1.6	42.8 ± 1.5
OST9	28.0 ± 2.3	43.6 ± 7.5	**OST23**	21.3 ± 1.5	23.5 ± 4.1
OST10	5.5 ± 3.3	-	**OST24**	29.0 ± 1.1	41.2 ± 4.2
OST11	44.5 ± 1.6	49.4 ± 5.1	**OST25**	36.5 ± 2.8	37.2 ± 4.1
OST12	43.5 ± 3.3	51.4 ± 4.1	**OST26**	NA	-

Table 2. Neuroprotection of compounds against H_2O_2 and OGD induced cytotoxity in SH-SY5Y cells

Compounds selected above were tested for their neuroprotection against oxygen glucose deprivation (OGD)-induced cell damage in SH-SY5Y cells. OGD model is also used to evaluate the cytoprotection of drugs against oxidative stress damage. The results were also listed in Table 2. Trends of cell viabilities were similar as in H_2O_2 model besides **OST14~16**. Pyridinamine structure seems more effective than phenyl amine structure in OGD model. But introducing pyridinamine could bring strong cytotoxicity during MTT assay (**OST11**, **OST13**). Thus, **OST4**, **OST6**, **OST7**, **OST8**, **OST9**, **OST12**, **OST17**, **OST22**, **OST24**, **OST25** were selected for next evaluation.

EC_{50} value of each compound was defined as the concentration that caused 50 % protective effect compare to the control group. Data listed in Table 3 are averages of three independent experiments, and expressed as mean ± SEM. As we can see, most compounds showed cytoprotective effects at low concentrations. **OST7** exhibited 50 % cytoprotective effect at 10.27 ± 0.54 and 3.27 ± 0.21 μM against H_2O_2 and OGD induced cytotoxity respectively in SH-SY5Y cells. We also obtained **OST12** and **OST17** that also exerted notable cytoprotective effects, with EC_{50} values of 16.61 ± 1.16 and 11.93 ± 1.36 μM against H_2O_2 induced cytotoxity and 9.05 ± 1.49 and 5.62 ± 0.65 μM against OGD induced cytotoxity. **OST4**, **OST9** and **OST24** showed higher values than osthole against H_2O_2. Especially **OST4** (> 100 μM), demonstrated again that introducing carbamates in this position could not bring a satisfactory bioactivity. **OST8** and **OST25** showed higher EC_{50} values than osthole against OGD, indicated that

though there are similarities in structure, introduction of piperazine can be more efficient than morpholine in cytoprotection.

Compd.	EC_{50} (H_2O_2) (μM)	EC_{50} (OGD) (μM)
Osthole	33.26 ± 0.25	26.45 ± 1.35
OST4	> 100	23.29 ± 0.56
OST6	29.84 ± 1.81	12.46 ± 1.08
OST7	10.27 ± 0.54	3.27 ± 0.21
OST8	27.52 ± 1.23	> 100
OST9	67.32 ± 2.21	15.29 ± 1.67
OST12	16.61 ± 1.16	9.05 ± 1.49
OST17	11.93 ± 1.36	5.62 ± 0.65
OST22	30.37 ± 2.27	13.28 ± 1.16
OST24	75.91 ± 2.38	18.84 ± 2.76
OST25	32.34 ± 1.22	40.05 ± 1.92

Table 3. EC_{50} values of selected compounds against H_2O_2 and OGD induced cytotoxity in SH-SY5Y cells

Inhibitory activities on LPS-induced NO production in RAW264.7 cell lines of the ten compounds mentioned above were illustrated in Table 4. **OST17** displayed better NO inhibitory ability than other selected derivatives. Compounds containing piperazine (**OST6**, **OST7**) and tetrahydropyrrole (**OST9**, **OST17**) group significantly inhibited NO production than compounds containing morpholine group (**OST8**, **OST12**). Though **OST22**, **OST24**, **OST25** did not offer satisfactory results in NO inhibition

when compared to other derivatives, modification as **OST22** did improve its original cytoprotective properties. It is worthwhile to further study columbianetin skeletons in neuroprotection.

Compd.	NO production (%) (10μM)
Control	10.2 ± 0.8
Indometacin	53.2 ± 6.2
Osthole	85.6 ± 13.3
OST4	77.4 ± 5.6
OST6	72.3 ± 5.6
OST7	62.8 ± 6.1
OST8	74.1 ± 11.3
OST9	75.4 ± 8.6
OST12	80.3 ± 9.1
OST17	50.4 ± 7.1
OST22	73.3 ± 6.5
OST24	106.2 ± 12.7
OST25	85.2 ± 8.3

Table 4. NO production activity of compounds against LPS induced RAW264.7 cells

Aβ is generated from the continuous processing of β-protease and γ-protease.[29] C-terminus of Aβ resulting from the processing of γ-protease, which digests at the transmembrane region of amyloid precursor protein (APP) and can produce a large number of 39~43 amino acid residue subtypes.[30] The most common residue subtypes are $A\beta_{40}$ and $A\beta_{42}$. Among the two, $A\beta_{40}$ is seen more commonly, but $A\beta_{42}$ relevant

more to the AD.[31] Cell viabilities of **OST7** and **OST17** against PC12 cells induced by $A\beta_{42}$ were performed by MTT assay were illustrated in Table 5. **OST7** displayed stronger neuroprotective activities at a low concentration of 1 μM and 10 μM.

Compd.	Concentration (μM)	Neuroprotection (%) (10μM)
Osthole	1	NA
	10	32.6 ± 2.2
	30	37.1 ± 3.6
OST7	1	55.2 ± 4.3
	10	61.4 ± 5.2
OST17	1	47.8 ± 4.8
	10	46.3 ± 3.9

Table 5. Neuroprotection of compounds against $A\beta_{42}$ induced cytotoxity in SH-SY5Y cells

Action mechanisms of **OST7** and **OST17** have been explored by computer modeling at the same time. Autodock vina was applied to calculate the possible binding method and affinity between $A\beta_{42}$ with **OST7** and **OST17**.[32] The 3D structure of $A\beta_{42}$ (1IYT) used was downloaded from the Protein Data Bank. As is observed in Figure 2, **OST7** binds to C-terminus region of the peptide in L-shape while **OST17** in U-shape binding gesture. **OST7** could form interactions with residues LEU34, GLY25, VAL24, ALA21 and PHE20. **OST17** could also form in a same distance with MET35, LEU34, ILE31, GLY25, VAL24 ALA21 and PHE20. During the aggregation of $A\beta_{42}$, a salt bridge is formed between K28 and E22 or D23 in the conformational change process.[33] An interaction with GLY25, VAL24 ALA21 and PHE20 might interrupt the production of

salt bridge, weaken the contraction between K28 and E22. The carbonyl group, isopentenyl group, and 1-acyl-4-boc piperazine structure can make **OST7** transform into a three-jaw configuration to better accommodate the surface of the α-helix of $A\beta_{42}$. As a result, the strong intermolecular interactions between **OST7** and $A\beta_{42}$ in the E22-K28 region would make this compound a promising molecule with potential $A\beta_{42}$ anti-aggregation activity.

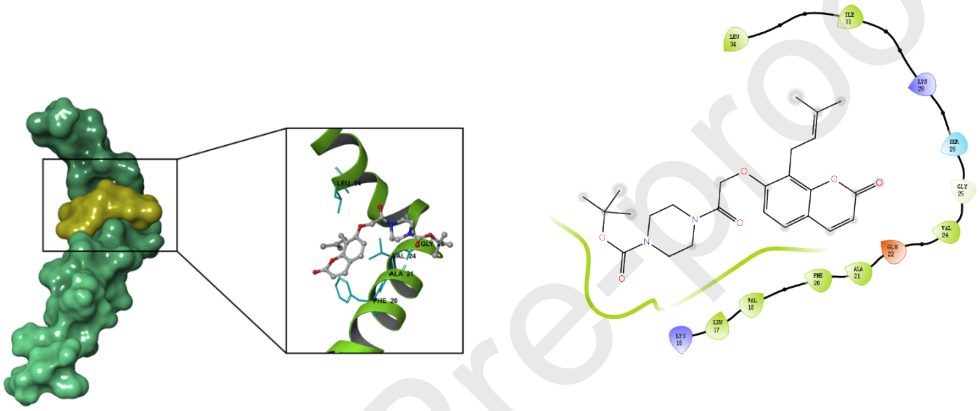

(A)

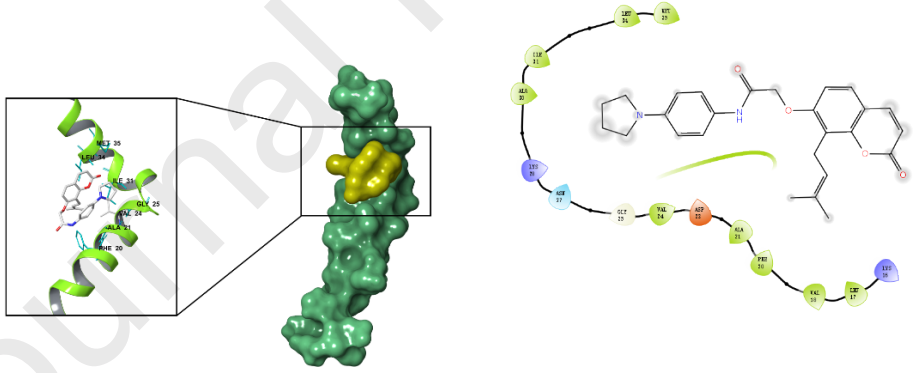

(B)

Figure 2. Predicted binding modes of compounds **OST7** (A) and **OST17** (B) with $A\beta_{42}$

In conclusion, A total of 26 compounds based on osthole were designed, synthesized. Their cytoprotective abilities of H_2O_2-induced, oxygen glucose deprivation-induced

neurotoxicity, LPS-induced NO production and $A\beta_{42}$-induced neurotoxicity were evaluated by MTT assays. Mechanism of the action of **OST7** and **OST17** were investigated by molecular docking. The structure activity relationship study indicated that introduction of piperazine-substituted carbamate and aromatic amine with tetrahydropyrrole into osthole can both increase its cytoprotective properties against H_2O_2 and OGD. Introduction of aromatic amine with tetrahydropyrrole structure as **OST17** added more NO inhibitive abilities to osthole. And molecular docking explained that the reason **OST7** exhibited stronger neuroprotection against Aβ because of the greater area of interactions between molecule and target protein. **OST7** and **OST17** both provided novel methods to investigate osthole as anti-AD drugs.

Acknowledgments

This work was supported by the National Natural Science Foundation of China (Grants 81973196 and 81673318), the 111 Project (Grant BP0719034) and the Natural Science Foundation of Shanghai (Grant 19ZR1413900).

Conflict of interest

We declare that we have no conflict of interest.

References

1. Burns A, Iliffe S. Alzheimer's disease. *Br Med J*. 2009, 338: 467-471.
2. Burns A, Bernabei R, Bullock R, et al. Safety and efficacy of galantamine (Reminyl)

222 in severe Alzheimer's disease (the SERAD study): a randomised, placebo-controlled,
223 double-blind trial. *Lancet Neurol*. 2009, 8(1): 39-47.
224 3. World Health Organization. Dementia fact sheet. World Health Organization:
225 Geneva, Switzerland. 2017.
226 4. Wilson RS, Aggarwal NT, Barnes LL, et al. Biracial population study of mortality
227 in mild cognitive impairment and Alzheimer disease. *Arch Neurol*. 2009, 66(6): 767-
228 772.
229 5. Alzheimer's Association. 2009 Alzheimer's disease facts and figures. *Alzheimer*
230 *Dement*. 2009, 5(3): 234-270.
231 6. Alzheimer's Association. 2017 Alzheimer's disease facts and figures. *Alzheimer*
232 *Dement*. 2017, 13(4): 325-373.
233 7. Reitz C, Mayeux R. Alzheimer disease: epidemiology, diagnostic criteria, risk
234 factors and biomarkers. *Biochem Pharmacol*. 2014, 88(4): 640-651.
235 8. Hardy JA, Higgins GA. Alzheimer's disease: the amyloid cascade hypothesis.
236 *Science*. 1992, 256(5054): 184-186.
237 9. Kamer AR, Craig RG, Dasanayake AP, et al. Inflammation and Alzheimer's
238 disease: possible role of periodontal diseases. *Alzheimer Dement*. 2008, 4(4): 242-250.
239 10. Mufson EJ, Counts SE, Perez SE, et al. Cholinergic system during the progression
240 of Alzheimer's disease: therapeutic implications. *Expert Rev Neurother*. 2008, 8(11):
241 1703-1718.
242 11. Schöneich C. Methionine oxidation by reactive oxygen species: reaction
243 mechanisms and relevance to Alzheimer's disease. *BBA-Proteins Proteom*. 2005,

1703(2): 111-119.

12. Akiyama H, Barger S, Barnum S, et al. Inflammation and Alzheimer's disease. *Neurobiol Aging*. 2000, 21(3): 383-421.

13. Shankar GM, Li S, Mehta TH, et al. Amyloid-β protein dimers isolated directly from Alzheimer's brains impair synaptic plasticity and memory. *Nat. Med.* 2008, 14(8): 837-842.

14. Alkam T, Nitta A, Mizoguchi H, et al. Restraining tumor necrosis factor-alpha by thalidomide prevents the amyloid beta-induced impairment of recognition memory in mice. *Behav Brain Res*. 2008, 189(1): 100-106.

15. Huang WC, Liao PC, Huang CH, et al. Osthole attenuates lipid accumulation, regulates the expression of inflammatory mediators, and increases antioxidants in FL83B cells. *Biomed Pharmacother*. 2017, 91: 78-87.

16. Chen T, Liu W, Chao X, et al. Neuroprotective effect of osthole against oxygen and glucose deprivation in rat cortical neurons: involvement of mitogen-activated protein kinase pathway. *Neuroscience*. 2011, 183: 203-211.

17. Xiao H, Jiao Y, Yan Y, et al. Osthole reduced Aβ synthesis by up-regulating miRNA-107 in neurons transfected with APP595/596 gene. *Chin Pharmacol Bull*. 2017, 33(8): 1079-1085.

18. Yang GX, Ge SL, Wu Y, et al. Design, synthesis and biological evaluation of 3-piperazinecarboxylate sarsasapogenin derivatives as potential multifunctional anti-Alzheimer agents. *Eur J Med Chem.* 2018, 156: 206-215.

19. Zhang C, Du QY, Chen LD, et al. Design, synthesis and evaluation of novel

266 tacrine-multialkoxybenzene hybrids as multi-targeted compounds against Alzheimer's
267 disease. *Eur J Med Chem*. 2016, 116: 200-209.
268 20. Pietrzycka A, Stępniewski M, Waszkiewicz AM, et al. Preliminary evaluation of
269 antioxidant activity of some 1-(phenoxyethyl)-piperazine derivatives. *Acta Pol Pharm.*
270 2006, 63(1): 19-24.
271 21. Hatnapure GD, Keche AP, Rodge AH, et al. Synthesis and biological evaluation
272 of novel piperazine derivatives of flavone as potent anti-inflammatory and
273 antimicrobial agent. *Bioorg Med Chem Lett*. 2012, 22(20): 6385-6390.
274 22. Venkatesh P, Pandeya SN. Synthesis, characterisation and anti-inflammatory
275 activity of some 2-amino benzothiazole derivatives. *Chemtech.* 2009, 1: 1354-1358.
276 23. Jeong HJ, Na HJ, Kim SJ, et al. Anti-inflammatory effect of columbianetin on
277 activated human mast cells. *Biol. Pharm. Bull*. 2009, 32(6): 1027-1031.
278 24. Zhang YB, Li W, Yang XW. Biotransformation of columbianadin by rat hepatic
279 microsomes and inhibition of biotransformation products on NO production in RAW
280 264.7 cells in vitro. *Phytochemistry.* 2012, 81: 109-116.
281 25. Ahn BN, Kim JA, Kong CS, et al. Protective effect of (20S)-columbianetin from
282 *Corydalis* heterocarpa on UVB-induced keratinocyte damage. *J Photoch Photobio B.*
283 2012, 109: 20-27.
284 26. Wood LG, Wark PA, Garg ML. Antioxidant and anti-inflammatory effects of
285 resveratrol in airway disease. *Antioxid Redox Sign*. 2010, 13(10): 1535-1548.
286 27. Zhang HR, Zhang HQ, Qu CL, et al. Fluorimetric and mass spectrometric study
287 of the interaction of β-cyclodextrin and osthole. *Spectrochim Acta A.* 2007, 68(3): 474-

477.

28. Lipinski CA, Lombardo F, Dominy BW, et al. Experimental and computational approaches to estimate solubility and permeability in drug discovery and development settings. *Adv Drug Delivery Rev.* 1997, 23(1-3): 3-25.

29. Leissring MA. The AβCs of Aβ-cleaving proteases. *J Biol Chem*. 2008, 283(44): 29645-29649.

30. Ledesma MD, Da Silva JS, Crassaerts K, et al. Brain plasmin enhances APP α-cleavage and Aβ degradation and is reduced in Alzheimer's disease brains. *EMBO Rep*. 2000, 1(6): 530-535.

31. Lehmann S, Delaby C, Boursier G, et al. Relevance of Aβ42/40 ratio for detection of Alzheimer disease pathology in clinical routine: the PLMR scale. *Front Aging Neurosci*. 2018, 10: 138.

32. Trott O, Olson AJ. AutoDock Vina: improving the speed and accuracy of docking with a new scoring function, efficient optimization and multithreading. *J Comput Chem*. 2010, 31: 455-461.

33. Melquiond A, Dong X, Mousseau N, et al. Role of the region 23-28 in Aβ fibril formation: insights from simulations of the monomers and dimers of Alzheimer's peptides $A\beta_{40}$ and $A\beta_{42}$. *Curr. Alzheimer Res*. 2008, 5: 244-250.

Highlights

- Twenty-six osthloe derivatives were designed and synthesized.
- Osthloe and its derivatives were investigated to evaluate the neuroprotective activity in four cell models.

- Molecular docking studies were further performed to explain possible binding poses to Aβ_{42} for the most promising analogs.
- Compounds **OST7** and **OST17** showed better activities and provided novel methods to investigate osthole as anti-AD drugs.